Investigation of the Goos-Hänchen shift in an optomechanical cavity via quantum control

Anwar Ali Khan,[1] Muqaddar Abbas,[2,*] You-Lin Chaung,[3] Iftikhar Ahmed,[1,4,†] and Ziauddin[2,3,‡]

[1]*Department of Physics, University of Malakand, Khyber Pakhtunkhwa, Pakistan*

[2]*Quantum Optics Lab, Department of Physics, COMSATS University, Islamabad, Pakistan*

[3]*Institute of Photonics and Technologies, National Tsing-Hua University, Hsinchu 300, Taiwan*

[4]*Gomal University, Dera Ismail Khan, Khyber Pakhtunkhwa, Pakistan*

(Received 23 March 2020; accepted 3 November 2020; published 18 November 2020)

We propose a scheme to study the topic of manipulating the Goos-Hänchen (GH) shift of the reflected beam in an optomechanical cavity (OMC). Our system consists of two mirrors where one is fixed and the other is movable and a two-level atom is trapped inside the OMC. The fixed mirror is partially reflecting, whereas the movable mirror is perfectly reflecting. We theoretically investigated the behavior of the GH shift in the reflected beam when a Gaussian beam is an incident on the OMC. We find that GH shifts can be greatly enhanced in positive or negative directions via manipulating the quantum parameters such as optomechanical strength $g_{\rm mc}$ and atom-cavity strength $g_{\rm ac}$ under the influence of beam width of a Gaussian beam. Besides, we study the GH shift in the case of the partially coherent light beam as an incident probe field. Giant negative GH shift is achieved for an incident partially coherent beam in the presence of $g_{\rm mc}$, $g_{\rm ac}$, a measure of global coherence and beam width of a partially coherent beam. The proposed model provides feasibility in practical experiments for studying the behavior of the GH shift.

DOI: 10.1103/PhysRevA.102.053718

I. INTRODUCTION

A tiny shift appearing when a light beam is totally reflected from an interface of two different media was first formulated by pitch [1]. After that, Goos and Hänchen experimentally observed this tiny lateral shift in the total internal reflection in 1947 [2]. It is of great interest in the applications of temperature-dependent optical sensors [3] and plasmon sensors which have high-resolution capability [4]. Consequently, the researchers pay great attention to investigating the behavior of the GH shift in different dispersive media. The positive GH shift has been studied in different structures such as total internal reflection [5], the interfaces between left and right-handed media [6], and multidimensional periodic structures [7]. Besides, the negative GH shift has been noticed in absorbing media [8] and atomic media with a negative index of refraction [9]. In general, the incident beam is considered as a Gaussian beam in the studies of GH shift [10], and the beam width plays a key role in both negative and positive shifts [10]. Further, the coherent effect also plays an important role in wave phenomena [10–15]. The problem of the GH shift with partially coherent light has been discussed in [16–20]. This paradox has been solved by Wang and co-workers first [21] and then by Ziauddin *et al.* [22]. In these works [21,22], it has been revealed that the measure of global coherence has a strong dependence on the GH shift.

Besides, the measurement of the GH shift in the optical regime is a tough job due to its small magnitude. Therefore, it is constructive to study the magnitude enhancement of the GH shift for the application point of view. Earlier, the magnitude enhancement of the GH shift has been studied theoretically and experimentally using several optical systems—these include, for example, absorptive medium [23], structural resonances [24], photonic crystal [25,26], metamaterials [27,28], metals [29,30], and a medium having negative refractive index [9]. Further, a considerable magnitude enhancement of the GH shift has been realized theoretically by varying the external parameters such as Kerr nonlinearity, spontaneously generated coherence, and parity-time symmetry [14,31,32].

On the other hand, cavity optomechanics [33,34] is an emerging field of research, in which the optical modes interact with the mechanical modes through radiation pressure and bring incredible progress in numerous fields of physics. In recent years, the cavity optomechanical phenomenon leads to numerous momentous applications, i.e., slow light in optomechanically induced transparency (OMIT) [35–41], atomic localization precision measurements [42,43], quantum information [44,45], manipulation of light propagation [46,47], squeezing of light [48], and strong coupling physics [49]. Cavity optomechanical systems possess various phenomena in electromagnetically induced transparency (EIT) [50], inverse EIT [51], Fano resonance [52], refractive index enhancement [53], and nanoscale optical cavities [38]. In the atomic configuration, multiple EIT can be obtained from the extension of a single EIT by incorporating numerous atomic systems, i.e., V-type [54], Y-type [55], N-type [56], and K-type [57] atomic media. The transmission of the probe field takes place in multiple EIT windows at different frequencies; this multiple

*muqaddarabbas@comsats.edu.pk
†ahma5532@gmail.com
‡ziauddin@comsats.edu.pk

EIT window has worthy contributions in optical communication processes where multichannel is functional and in the optical processing. In OMC, a double OMIT window has been explored in a charged optomechanical system [58], coupled disks structure [59], coupled OMC [60], and double resonators OMC [61,62].

Further, the hybrid atom-cavity quantum systems have revealed a substantial amount of research in this decade [63,64]. Two well-established fields such as cavity quantum electrodynamics [65] and quantum optomechanics [66] are expected to be a fundamental part of future quantum technologies. In these systems, a lot of phenomena can be generated due to light-mechanical interaction and atom-light interaction at the quantum level. Earlier, the hybrid cavity systems have been investigated theoretically [67,68] and experimentally [69,70]. In these hybrid systems, a mechanical oscillator interacts simultaneously with matter (like single or multilevel systems such as Bose-Einstein condensate) and radiation field that can be used in many phenomena of pure quantum nature. Very recently, an OMC has been considered and investigated in the GH shift for the reflected beam by using a plane wave [71]. It is a fascinating phenomenon to demonstrate the classical nature of the GH shift depending on the quantum nature of the cavity parameters.

In the current work, we proceed with the investigation as studied in Ref. [71] and consider an OMC in which a two-level atom is trapped inside it. When a single atom is trapped inside the optomechanical cavity, then it couples to the cavity field by dipole interaction and the cavity optomechanics combines with the cavity quantum electrodynamics. As a result, there is a strong coupling between a single trapped atom and optomechanical oscillator [67,68]. A related and significant question in the framework of such a hybrid system is what kind of effect on the GH shift can be achieved when there are cavity-mechanics and atom-cavity coherent interaction? In this article, we try to answer this question theoretically in such a hybrid system and deal with two quantum parameters such as optomechanical strength $g_{\rm mc}$ and atom-cavity strength $g_{\rm ac}$. Further, the GH shift is very tiny, i.e., several optical wavelengths, so that its measurement becomes a difficult task. On the other hand, how to estimate the coupling strength between an interacting cavity field and the atomic system as well as the coupling between the cavity field and optomechanical system is the other difficult task in the experiment. To solve the two problems simultaneously, here, we have proposed the hybrid system which consists of a two-level atom inside an optomechanical system. We expect that the GH shift can be amplified in the presence of the trapping atom, while the coupling strengths of atom cavity and optomechanical can be highlighted due to the observable shift. With the study of this hybrid system, we can estimate the physical coupling strength which is crucial to the atomic physics and other realm related to light-matter interactions. Our proposed model provides an accessible way to measure the coupling strengths by the amplified GH shift which can be easily observed in practical experiments. We also know that the quantum parameters affect the behavior of the output probe field as studied earlier [61,62]. It will be more interesting if we consider a probe beam is a Gaussian or partially coherent beam instead of a plane wave and study the behavior of the GH shift in the reflected beam in the proposed hybrid system.

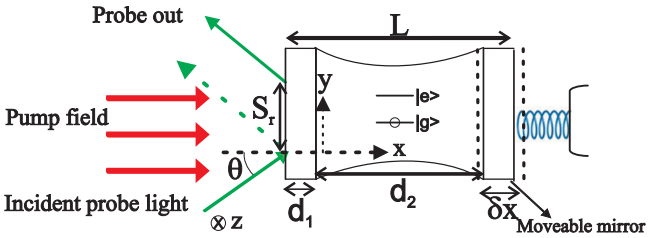

FIG. 1. System of OMC interacting with probe and coupling fields. A Fabry-Pérot cavity length is L. It consists of a stationary mirror, moving mirror, and a two-level atom contained inside the cavity. The thickness of the left mirror and the length of the cavity are denoted by d_1 (permittivity ϵ_1) and d_2 (effective permittivity ϵ_2), whereas δx is the mean displacement of moving mirror and S_r is the lateral shift in the reflected probe beam. At the same time, the cavity is impinged by weak probe field $\omega_{\rm p}$ at an incident angle θ and strong pump field $\omega_{\rm l}$ is denoted by arrows normal to the stationary mirror.

II. MODEL

The system is composed of a two-level atom trapped inside a Fabry-Pérot OMC whose length is L as shown in Fig. 1. The cavity consists of two mirrors where one is partially reflected and the other is perfectly reflected. The perfect reflected mirror is movable, whereas the other mirror is fixed. The nonlinear coupling is directly coming from the optomechanical effect, and the two-level atomic system can be dealt with the Jaynes-Cummings (JC) model [72]. We consider a strong pump field with frequency $\omega_{\rm l}$ and a weak probe field with frequency $\omega_{\rm p}$ interacting with the OMC. In the scenario, the Hamiltonian of the system can be represented as [73]

$$H = \left(\frac{p^2}{2m} + \frac{m\omega_{\rm m}^2 x^2}{2}\right) + \hbar\Delta_{\rm c} c^\dagger c + \hbar\frac{\Delta_{\rm a}}{2}\sigma_{\rm z} - \hbar g_{\rm mc} c^\dagger c x + \hbar g_{\rm ac}(c^\dagger\sigma_1 + c\sigma_1^\dagger) + i\hbar\mathcal{E}_{\rm l}(c^\dagger - c) + i\hbar\mathcal{E}_{\rm p}(c^\dagger e^{-i\delta t} - e^{i\delta t} c). \quad (1)$$

Here, $\Delta_{\rm c} = \omega_{\rm c} - \omega_{\rm l}$, $\Delta_{\rm a} = \omega_{\rm a} - \omega_{\rm l}$, and $\delta = \omega_{\rm p} - \omega_{\rm l}$ are the detunings of cavity field frequency, atomic transition frequency, and the probe field frequency with respect to the pump field frequency, respectively. ω_c and ω_a are the cavity resonance and atomic transition frequencies, respectively. In Eq. (1), the first term is the Hamiltonian of a moving mirror having mass m and frequency $\omega_{\rm m}$, and the position and momentum operators of the oscillator are represented by x and p. The second term defines the self-energy of cavity mode, where $c^\dagger$ and c are the corresponding creation and annihilation operators. The third term describes the Hamiltonian of the two-level atomic system whose resonant frequency is given by ω_a. $\sigma_{\rm z}$ represents the Pauli-spin matrices of the two-level atom. The fourth term represents the interaction of cavity mode and oscillating mirror, where $g_{\rm mc}$ is the quantum parameter and is known as optomechanical strength. The fifth term is the interaction Hamiltonian between the two-level atom and cavity mode, where $g_{\rm ac}$ is the other quantum parameter. $\sigma_1^\dagger = \frac{\sigma_{\rm x} + i\sigma_{\rm y}}{2}$ and $\sigma_1 = \frac{\sigma_{\rm x} - i\sigma_{\rm y}}{2}$ are the creation and destruction

operators of the two-level atom. The last two terms in Eq. (1) represent the interactions between cavity mode with a strong pump and a weak probe field which have Rabi frequencies ω_l and ω_p, respectively. The field amplitude of pump and probe field are given as $|\mathcal{E}_l| = \sqrt{2\kappa P_l/\hbar\omega_l}$ and $|\mathcal{E}_p| = \sqrt{2\kappa P_p/\hbar\omega_p}$, where P_l and P_p are the input power of pump and probe field with the corresponding frequencies ω_l and ω_p. κ is the cavity decay rate. In the following, we examine the time evolution of the optomechanical system and use the Heisenberg operator method whose general expression can be written as

$$\frac{dA}{dt} = -\frac{i}{\hbar}[A, H]. \tag{2}$$

According to the system Hamiltonian as given in Eq. (1), we can obtain the Heisenberg equations of motion using Eq. (2) as

$$\begin{aligned}
\ddot{x} &= -\omega_m^2 x + \gamma_m \dot{x} + \frac{\hbar g_{mc}}{m} c^\dagger c, \\
\dot{c} &= -(\kappa + i\Delta_c)c + i g_{mc} c x - i g_{ac}\sigma_1 + \mathcal{E}_l + \mathcal{E}_p e^{-i\delta t} \\
&\quad + \sqrt{2\kappa}\, c_{in}(t), \\
\dot{\sigma_1} &= -(\gamma_a + i\Delta_a)\sigma_1 + i g_{ac} c \sigma_z + \sqrt{2\gamma_a}\, a_{in}(t),
\end{aligned} \tag{3}$$

where γ_a represents the damping rate of an atom and γ_m shows the decay rate of mechanical mode. We have also presented the input vacuum noises related to the cavity field $c_{in}(t)$ and atom $a_{in}(t)$, respectively. The mean values of $c_{in}(t)$ and $a_{in}(t)$ become equal to zero, i.e., $\langle c_{in}(t)\rangle = \langle a_{in}(t)\rangle = 0$. The nonvanishing commutation relations are given as $\langle c_{in}(t) c_{in}^\dagger(t')\rangle = \delta(t - t')$ and $\langle a_{in}(t) a_{in}^\dagger(t')\rangle = \delta(t - t')$. Taking the average of the above three equations, we get

$$\begin{aligned}
\langle \dot{x}\rangle &= \frac{\langle p\rangle}{m}, \\
\langle \ddot{x}\rangle &= -\omega_m^2\langle x\rangle - \gamma_m\langle \dot{x}\rangle + \frac{\hbar g_{mc}}{m}\langle c^\dagger\rangle\langle c\rangle, \\
\langle \dot{c}\rangle &= -(\kappa + i\Delta_c)\langle c\rangle + i g_{mc}\langle c\rangle\langle x\rangle - i g_{ac}\langle\sigma_1\rangle \\
&\quad + \mathcal{E}_l + \mathcal{E}_p e^{-i\delta t}, \\
\langle \dot{\sigma_1}\rangle &= -(\Gamma_a + i\Delta_a)\langle\sigma_1\rangle + i g_{ac}\langle c\rangle\langle\sigma_z\rangle.
\end{aligned} \tag{4}$$

For a low excitation limit, we consider $\langle\sigma_z\rangle = \langle\sigma_z\rangle_{ss} = -1$. In order to get a steady-state solution of the above equation, we use an ansatz as

$$\begin{aligned}
\langle x\rangle &= x_s + x_- e^{-i\delta t} + x_+ e^{i\delta t}, \\
\langle c\rangle &= c_s + c_- e^{-i\delta t} + c_+ e^{i\delta t}, \\
\langle\sigma_1\rangle &= \sigma_{1s} + \sigma_{1-} e^{-i\delta t} + \sigma_{1+} e^{i\delta t},
\end{aligned} \tag{5}$$

where $i_s(x, c, \sigma)$ are known as the steady-state solution. Using the above ansatz, we obtain the steady-state solution as follows:

$$\begin{aligned}
x_s &= \frac{\hbar g_{mc}|c_s|^2}{m\omega_m^2}, \\
c_s &= \frac{\mathcal{E}_l}{\kappa + i\Delta' - \frac{g_{ac}^2\langle\sigma_z\rangle_{ss}}{\gamma_a + i\Delta_a}}.
\end{aligned} \tag{6}$$

From Eqs. (4) and (5), we can obtain the expression as

$$c_- = \left(\frac{\beta_5\beta_1 g_{ac}^2 m - i\beta_2\beta_5 g_{mc}^2 c_s c_s^* - \beta_1\beta_2\beta_3\beta_5 m}{A + B + C}\right)\mathcal{E}_p, \tag{7}$$

where

$$\begin{aligned}
\Delta' &= \Delta_c - g_{mc}x_s, \\
A &= \beta_1 g_{ac}^4 m + \beta_1\beta_4\beta_5 g_{ac}^2 m - \beta_1\beta_3\beta_2 g_{ac}^2 m, \\
B &= -\beta_1\beta_2\beta_3\beta_4\beta_5 m - i\beta_5 g_{ac}^2 g_{mc}^2 c_s c_s^* - i\beta_5 c_s c_s^* g_{ac}^2 g_{mc}^2, \\
C &= -i\beta_2\beta_4\beta_5 m g_{mc}^2 c_s c_s^* + i\beta_2\beta_3\beta_5 g_{mc}^2 c_s c_s^*, \\
\beta_1 &= -\delta^2 - i\delta\gamma_a + \omega_m^2, \\
\beta_2 &= -i\delta + \gamma_a - i\Delta_a, \\
\beta_3 &= -i\delta - i\Delta' + \kappa, \\
\beta_4 &= -i\delta + \Delta' + \kappa, \\
\beta_5 &= -i\delta + \gamma_a + i\Delta_a.
\end{aligned} \tag{8}$$

The input-output relation of the cavity may be written as [35,74]

$$E_{out}(t) + \mathcal{E}_p e^{-i\delta t} + \mathcal{E}_l = \sqrt{2\kappa}\, c, \tag{9}$$

where

$$E_{out}(t) = E_{out}^0 + E_{out}^+\mathcal{E}_p e^{-i\delta t} + E_{out}^-\mathcal{E}_p e^{i\delta t}. \tag{10}$$

After solving Eqs. (8)and (9), we obtain the relation as

$$E_{out}^+ = \frac{\sqrt{2\kappa}\, c_-}{\mathcal{E}_p} - 1, \tag{11}$$

that can be measured by using the homodyne technique [74]. For convenience, we define

$$E_{out}^+ + 1 = \frac{\sqrt{2\kappa}\, c_-}{\mathcal{E}_p} = \mathcal{E}_T. \tag{12}$$

The quadratures of the field $\mathcal{E}_T$ can be defined as $\mathcal{E}_T = u_p + iv_p$. Here, u_p and v_p are the in-phase and out-of-phase quadratures of the output probe field, respectively. The u_p and v_p represent the absorptive and dispersive behavior of the probe field through the cavity, respectively.

The OMC consists of two nonconducting mirrors in which the left mirror M_1 is fixed and partially reflecting and the right mirror M_2 is movable and perfectly reflecting. We define d_i and ϵ_i as the thickness and permittivity of M_i, $i \in 1, 2$. The permittivity of the dielectric slabs (ϵ_1) remained fixed, while the permittivity of the intracavity medium (ϵ_2) is connected to the $\mathcal{E}_T$ of the cavity via the relation

$$\epsilon_2 = 1 + \mathcal{E}_T. \tag{13}$$

To study the behavior of the GH shift in the reflected beam in the optomechanical system, we consider two cases: a Gaussian-shaped probe beam and a partially coherent probe beam.

A. Incident Gaussian beam

When a Gaussian probe beam is incident upon an OMC from left, the incident probe Gaussian beam can be

expressed as

$$E_z^i(x,y) = \frac{1}{\sqrt{2\pi}} \int E(k_y) e^{i(k_x x + k_y y)} dk_y, \tag{14}$$

where $E(k_y) = \frac{w_y}{\sqrt{2\pi}} e^{\frac{-w_y^2 (k_y - k_{y0})^2}{4}}$ is known as the angular spectrum of the probe Gaussian beam centered at $y = 0$ of the plane of $x = 0$, $k_{y0} = k \sin\theta$, and $w_y = w_s \sec\theta$, where θ is the incident angle and w_s is the half beam width. The mathematical expression for the reflected beam can be expressed as [10,75]

$$E_z^r(x,y)|_{x<0} = \frac{1}{\sqrt{2\pi}} \int r(k_y) E(k_y) e^{i(-k_x x + k_y y)} dk_y, \tag{15}$$

where $r(k_y)$ is the reflection coefficient which can be calculated using a transfer matrix equation [10,75].

For a Gaussian incident beam with a narrow width, the GH shift S_r is defined as [10,75]

$$S_r = \frac{\int_{-\infty}^{\infty} y |E_z^r(x,y)|^2 dy}{\int_{-\infty}^{\infty} |E_z^r(x,y)|^2 dy}. \tag{16}$$

B. Incident partially coherent beam

In the real circumstances, when the incident beams are partially coherent, the fields contain fluctuations both in-phase and amplitude. It means that for a reflected field there is no definite phase. To understand the partially coherent light, we consider two-dimensional partially coherent fields. We use the cross-spectral density function $W(y_1, x_1; y_2, x_2)$, which describes the propagation of the partially coherent field. Here, (y_1, x_1) and (y_2, x_2) show two points in the fields. Using Mercer's expansion, we can represent the cross-spectral density function as [21,76]

$$W(y_1, x_1; y_2, x_2) = \sum \beta_n \psi_n^*(y_1, x_1) \psi_n(y_1, x_1), \tag{17}$$

where ψ_n and β_n are the eigenfunctions and eigenvalues, respectively. The partially coherent fields can be explained more precisely by using a Gaussian shell-model beam [21,76]. The normalized eigenfunctions and eigenvalues of a Gaussian shell-model beam can be written as [21,76]

$$\psi_n(y) = (2c/\pi)^{1/4} \frac{1}{\sqrt{2^n n!}} H_n[y\sqrt{2c}] e^{-cy^2} \tag{18}$$

and

$$\beta_n = A^2 [\pi/(a+b+c)]^{1/2} [b/(a+b+c)]^n, \tag{19}$$

where H_n are the Hermite polynomials, whereas $a = (4w_s^2)^{-1}$, $b = (2w_g^2)^{-1}$, and $c = [a^2 + 2ab]^{1/2}$. The final expression of c can be achieved as $c = (q^2+4)^{1/2}/(4qw_s^2 \sec^2\theta)$ by choosing $w_s \to w_s \sec\theta$ and $w_g \to w_g \sec\theta$, where $q = w_g/w_s$ shows the measure of global coherence. It is emphasized that the angular spectrum $\psi_n(k_y)$ can be derived from Eq. (18) by taking its Fourier transform. For an inclined incidence, $\psi_n(k_y)$ can be expressed as $\psi_n(k_y - k_{y_0})$, where k_y represents the y component of k and $k_{y_0} = k \sin\theta$. For nth mode, the reflected beam can be calculated as [21]

$$\psi_n^r(y) = \frac{1}{\sqrt{2\pi}} \int r(k_y) \psi_n(k_y - k_{y_0}) e^{ik_y y} dk_y, \tag{20}$$

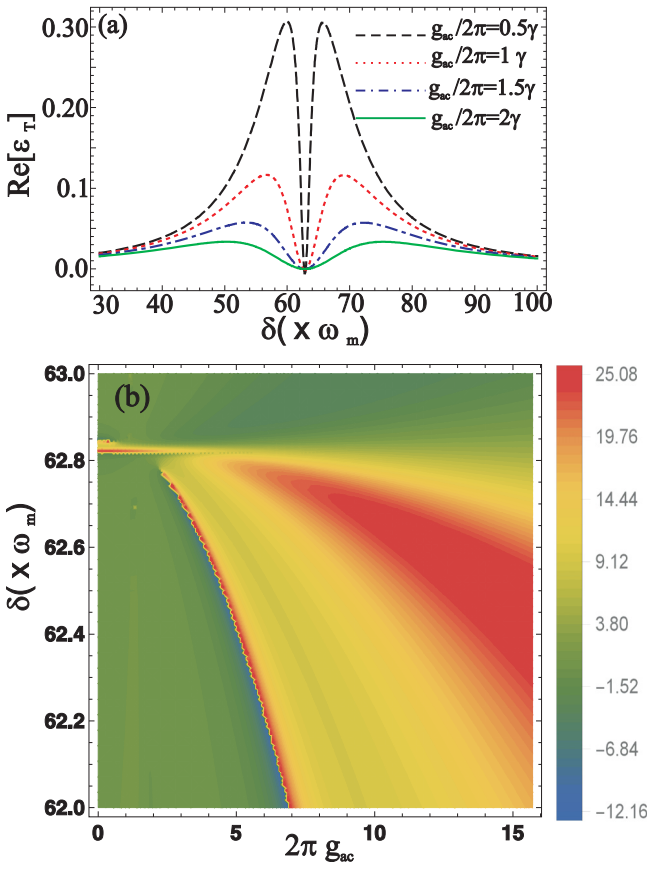

FIG. 2. (a) Re[$\mathcal{E}_T$] vs probe field detuning δ by considering $g_{mc} = \gamma$. (b) Density plot of the GH shift vs probe field detuning δ and g_{ac} by considering $\theta = 0.14$ rad, $g_{mc} = \gamma$, and $w_s = 5\lambda$. The other parameters are $\epsilon_0 = 1$, $\epsilon_1 = 2.22$, $d_1 = 0.2$ μm, $d_2 = 5$ μm, $\gamma = 1$ MHz, $\mathcal{E}_l/2\pi = 0.5\gamma$, $P_l = 4.9$ μW, $\omega_m/2\pi = 10\gamma$, $\Delta_a/2\pi = 10\gamma$, $\gamma_a/2\pi = 0.002\gamma$, $\Gamma_m/2\pi = 0.000\,141\gamma$, and $\kappa = \omega_m/10$.

where

$$\psi_n(k_y - k_{y_0}) = \frac{1}{(2c\pi)^{1/4}} \frac{(-i)^n}{\sqrt{2^n n!}} e^{\frac{(k_y - k_{y_0})^2}{4c}} H_n\left(\frac{(k_y - k_{y_0})}{\sqrt{2c}}\right). \tag{21}$$

When partially coherent fields are reflected at the interface between two media, then each mode n experiences a lateral shift as [21]

$$S_n^r = \frac{\int y |\psi_n^r(y)|^2 dy}{\int |\psi_n^r(y)|^2 dy}. \tag{22}$$

III. RESULTS AND DISCUSSION

A. Interaction of incident Gaussian beam with an OMC

We start with the discussion of the GH shift of Gaussian beam in the presence of the two-level atom. We show the spectrum of OMIT (Re[$\mathcal{E}_T$]) versus probe field detuning for different values of g_{ac}; see Fig. 2(a). We find a narrow transparency window appears for a small value of g_{ac} (black dashed curve). The transparency window becomes broader when the value of g_{ac} increases; see the red dotted, blue dashed dotted, and green solid curves in Fig. 2(a). In the presence of g_{ac} the effective loss of the cavity decreases, which leads to enhanced

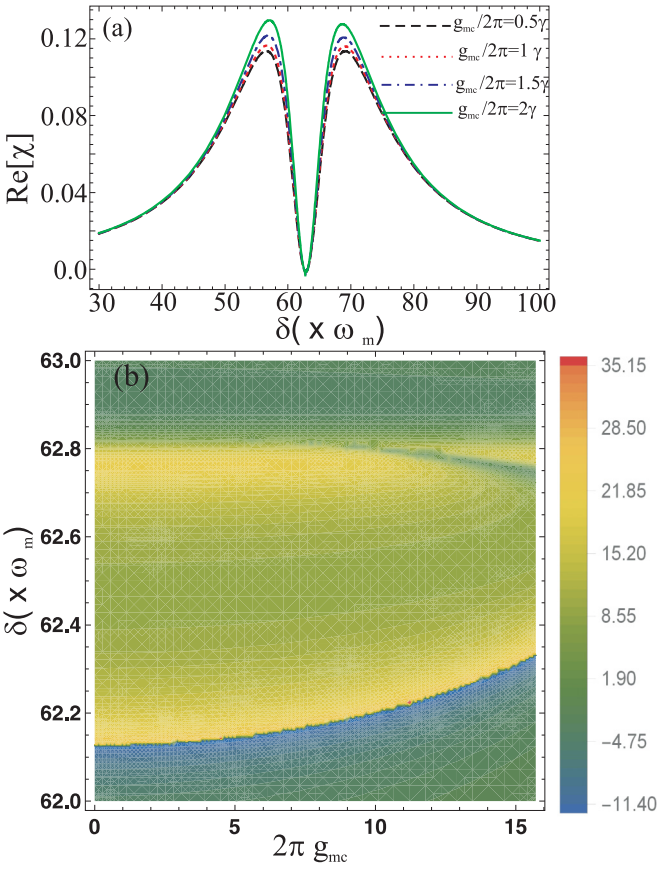

FIG. 3. (a) Re[$\mathcal{E}_T$] vs probe field detuning δ by considering $g_{ac} = \gamma$. (b) Density plot of the GH shift vs probe field detuning δ and g_{mc} by considering $\theta = 0.14$ rad, $g_{ac} = \gamma$, and $w_s = 5\lambda$. The other parameters are $\epsilon_0 = 1$, $\epsilon_1 = 2.22$, $d_1 = 0.2$ μm, $d_2 = 5$ μm, $\gamma = 1$ MHz, $\mathcal{E}_l/2\pi = 0.5\gamma$, $P_l = 4.9$ μW, $\omega_m/2\pi = 10\gamma$, $\Delta_a/2\pi = 10\gamma$, $\gamma_a/2\pi = 0.002\gamma$, $\Gamma_m/2\pi = 0.000\,141\gamma$, and $\kappa = \omega_m/10$.

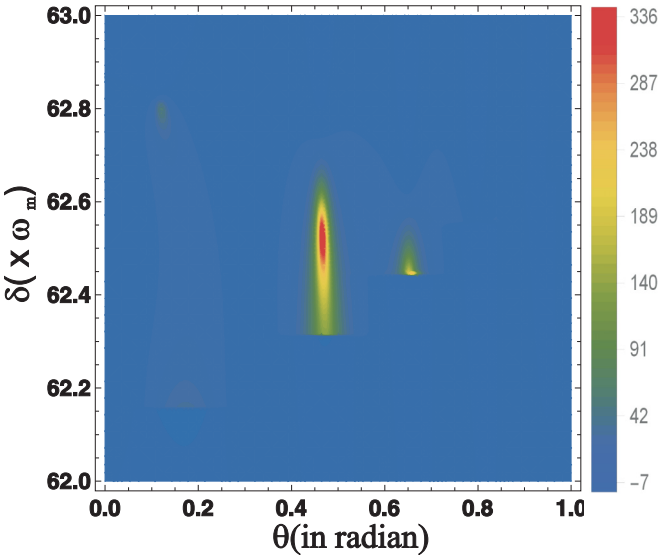

FIG. 4. Contour plot of the GH shift vs probe field detuning δ and θ by considering $g_{mc} = g_{ac} = \gamma$ and $w_s = 5\lambda$. The other parameters are $\epsilon_0 = 1$, $\epsilon_1 = 2.22$, $d_1 = 0.2$ μm, $d_2 = 5$ μm, $\gamma = 1$ MHz, $\mathcal{E}_l/2\pi = 0.5\gamma$, $P_l = 4.9$ μW, $\omega_m/2\pi = 10\gamma$, $\Delta_a/2\pi = 10\gamma$, $\gamma_a/2\pi = 0.002\gamma$, $\Gamma_m/2\pi = 0.000\,141\gamma$, and $\kappa = \omega_m/10$.

radiation pressure [77]. Therefore, in the presence of g_{ac}, together with g_{mc} influences the OMIT that can modify strongly the GH shift. To study the GH shift we consider a Gaussian probe beam incident on an OMC from left making an angle θ with x axis. We are interested in studying the manipulation of the GH shift using quantum parameters such as cavity optomechanical strength g_{mc} and atom-cavity strength g_{ac}. Initially, we study the dependence of the GH shift upon the probe field detuning δ. We show a contour plot of the GH shift versus δ with g_{ac} by considering the incident angle $\theta = 0.14$ radian using Eq. (15) as shown in Fig. 2(b). It is also emphasized that the OMIT or the transparency window can be achieved in our model at around $\delta = 62.82\gamma$. The plot in Fig. 2(b) shows that the magnitude of the GH shift varies with increasing the strength of g_{ac}. The magnitude of the GH shift is large and positive at $\delta = 62.82\gamma$ for small values of g_{ac}. It is because the OMIT in our system is very narrow for small values of g_{ac}. When the value of g_{ac} increases, the width of the OMIT window increases and, in that case, we can choose any other values for δ instead of $\delta = 62.82\gamma$. Therefore, Fig. 2(b) shows that we get negative and positive shifts for different values of g_{ac} and δ. The magnitude of the GH shift changes by changing the probe field detuning and g_{ac}. Further, the width of OMIT remains unchanged with increasing the strength of g_{mc} under the presence of g_{ac}, as shown in Fig. 3(a). We find there is a transparency window for a small value of g_{mc} (black dashed curve) and it remains the same with the increment of g_{mc}; see the red dotted, blue dashed dotted, and green solid curves in Fig. 3(a). In the presence of g_{ac}, we show the spectrum of the GH shift in the reflected beam versus δ and g_{mc}, while all the other parameters are unchanged; see Fig. 3(b). We get a negative and positive GH shifts for different pairs of δ and g_{mc}. This means that the other quantum parameter, i.e., g_{mc}, also affects the magnitude of the GH shift. To extend the discussion further, we study how the GH shift changes with the probe field detuning and incident angle varies. In Fig. 4, we show a contour plot of the GH shift versus δ and θ. Enhanced positive GH shift is achieved at incident angle $\theta = 0.46$ radian and $\delta = 62.5\gamma$ in the presence of quantum parameters g_{mc} and g_{ac}. At the same incident angle $\theta = 0.46$ radian, the magnitude of the GH shift varies with the variation of probe field detuning δ. We also find positive GH shift at some other incident angles and probe field detuning.

Very recently, the influence of the quantum parameter g_{mc} on the GH shift has been studied and developed so that it affects the behavior of the GH shift [71]. In the present section, we consider the optomechanical system having an atom inside it and using a Gaussian incident probe beam. In the proposed system, we have two quantum parameters such as optomechanical strength g_{mc} and atom-cavity strength g_{ac}. We expect that the two quantum parameters must affect the behavior of the GH shift. To investigate the influence of the quantum parameters on the GH shift, next, we study the influence of the quantum parameter g_{mc} on the GH shift in the absence of another quantum parameter g_{ac}. We show a contour plot of the GH shift versus incident angle θ and g_{mc} as depicted in Fig. 5(a). The plot shows that, at $g_{mc} = 0$ or approaching zero,

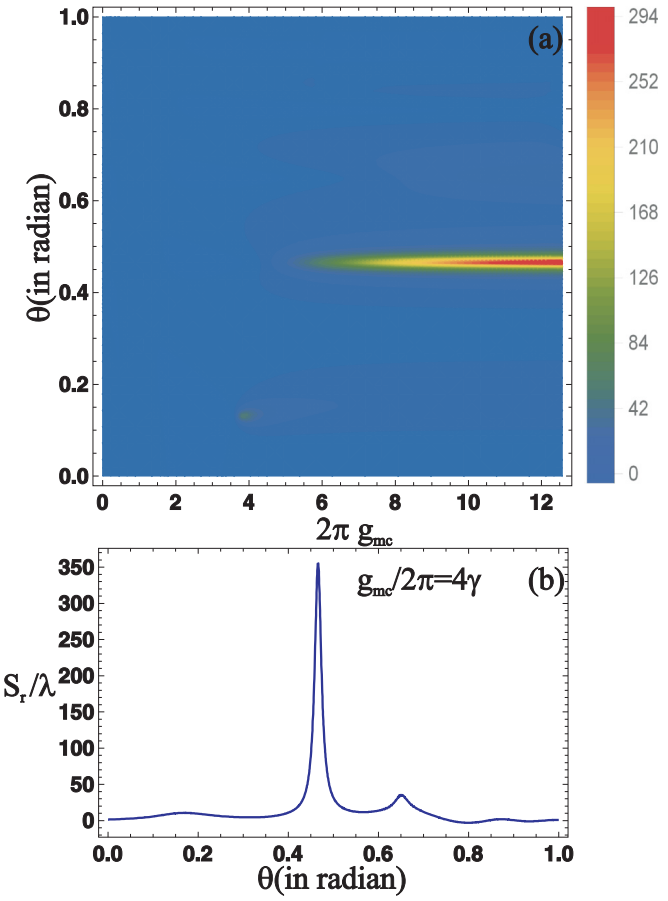

FIG. 5. (a) Contour plot of the GH shift vs incident angle θ and $g_{\rm mc}$ by considering $g_{\rm ac} = 0$ and $w_s = 5\lambda$; (b) the GH shift vs incident angle θ. The other parameters are $\epsilon_0 = 1$, $\epsilon_1 = 2.22$, $d_1 = 0.2\ \mu$m, $d_2 = 5\ \mu$m, $\gamma = 1$ MHz, $\mathcal{E}_l/2\pi = 0.5\gamma$, $P_1 = 4.9\ \mu$W, $\omega_m/2\pi = 10\gamma$, $\Delta_a/2\pi = 10\gamma$, $\gamma_a/2\pi = 0.002\gamma$, $\Gamma_m/2\pi = 0.000\,141\gamma$, and $\kappa = \omega_m/10$.

the magnitude of the GH shift is zero at different incident angles. Positive GH shifts appear at different choices of incident angles. It is found that the enhanced positive GH shift appears at $\theta = 0.46$ radian. It is also investigated that the GH shift at $\theta = 0.46$ radian starts from $2\pi g_{\rm mc} = 5.4\gamma$ or $g_{\rm mc} = 0.86\gamma$. For further increase in the strength of the $g_{\rm mc}$, the magnitude of the GH shift increases as shown in Fig. 5(b). The plot shows that the magnitude of the GH shift increases more slightly beyond $2\pi g_{\rm mc} = 12\gamma$. A saturation occurs when we double the value of $2\pi g_{\rm mc} = 24\gamma$.

Further, the quantum parameter $g_{\rm ac}$ can also affect the behavior of the OMIT in the cavity system. Therefore, it is expected that it can also influence the GH shift as well. In the absence of $g_{\rm mc}$, we show a contour plot of the GH shift versus incident angle θ and $g_{\rm ac}$ as shown in Fig. 6. The plot shows that, in the absence of optomechanical strength $g_{\rm mc}$, the GH shift can be flexibly manipulated via atom-cavity strength $g_{\rm ac}$. It is found that the magnitude of the GH shift is maximum for small values of $g_{\rm ac}$ at different incident angles. The maximum GH shift appears at incident angle $\theta \approx 0.39$ radian with $2\pi g_{\rm ac} \approx 0.892\gamma$ or $g_{\rm ac} \approx 0.14\gamma$. Similarly, an enhanced GH shift is also achieved at an incident angle $\theta \approx 0.56$ radian with

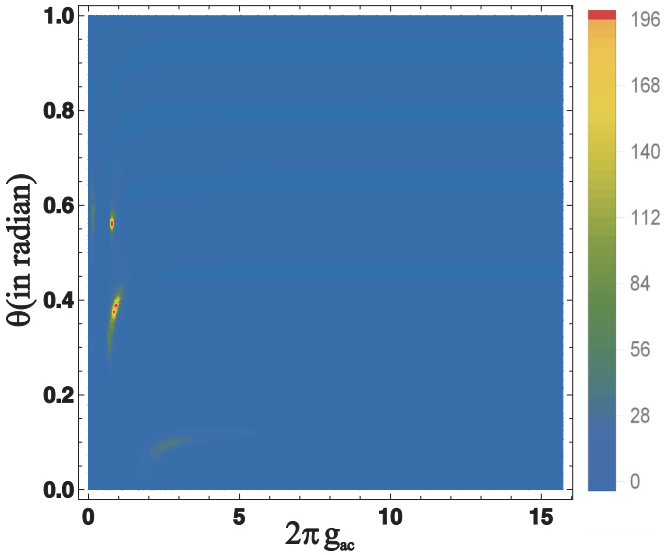

FIG. 6. Contour plot of the GH shift vs incident angle θ and $g_{\rm ac}$ by considering $g_{\rm mc} = 0$ and $w_s = 5\lambda$; the other parameters are $\epsilon_0 = 1$, $\epsilon_1 = 2.22$, $d_1 = 0.2\ \mu$m, $d_2 = 5\ \mu$m, $\gamma = 1$ MHz, $\mathcal{E}_l/2\pi = 0.5\gamma$, $P_1 = 4.9\ \mu$W, $\omega_m/2\pi = 10\gamma$, $\Delta_a/2\pi = 10\gamma$, $\gamma_a/2\pi = 0.002\gamma$, $\Gamma_m/2\pi = 0.000\,141\gamma$, and $\kappa = \omega_m/10$.

$2\pi g_{\rm ac} \approx 0.74\gamma$ or $g_{\rm ac} \approx 0.11\gamma$. In the absence of $g_{\rm mc}$, we get large GH shift for small values of $g_{\rm ac}$ and vice versa. This is due to the fact that the total group index of the cavity increases for small values of $g_{\rm ac}$ and vice versa. The magnitude of the GH shift is dependent on the total group index of the medium which has been reported earlier [12]. From the above investigation, we can safely conclude that the magnitude of the GH shift can be manipulated via atom-cavity strength.

It has been established earlier that the beam width of a Gaussian beam influences the behavior of the GH shift by considering the atomic medium in a cavity [10]. It is now constructive to study the influence of beam width of the Gaussian beam on the GH shift in an OMC. We choose a fixed incident angle and plot the GH shift versus beam width under the influence of quantum parameters. First, we consider the incident angle $\theta = 0.46$ radian, $g_{\rm mc}/2\pi = 1.5\gamma$, and $g_{\rm ac} = 0$ and show a spectrum of the GH shift as depicted in Fig. 7(a). We get a positive GH shift, where its magnitude becomes maximum at around $w_s = 5\lambda$ and, for further increase in the beam width of a Gaussian beam, the magnitude of the positive GH shift decreases. Further, in the presence of $g_{\rm ac}$ and $g_{\rm mc}$, we show a spectrum of the GH shift vs beam width where all the other parameters remain the same as that in Fig. 7(a). The spectrum of the GH shift in the reflected beam is shown in Fig. 7(b). Under the influence of both the quantum parameters, we get negative GH shifts for different choices of beam width of the Gaussian beam. The maximum negative GH shift is achieved for beam width $w_s = 12.5\lambda$; see Fig. 7(b). Here, the quantum parameter $g_{\rm ac}$ switches the GH shift from positive to negative at incident angle $\theta = 0.46$ radian.

B. Interaction of incident partially coherent beam with an OMC

Earlier, the GH shift has been investigated for a partially coherent light using different media [21,22]. In the following

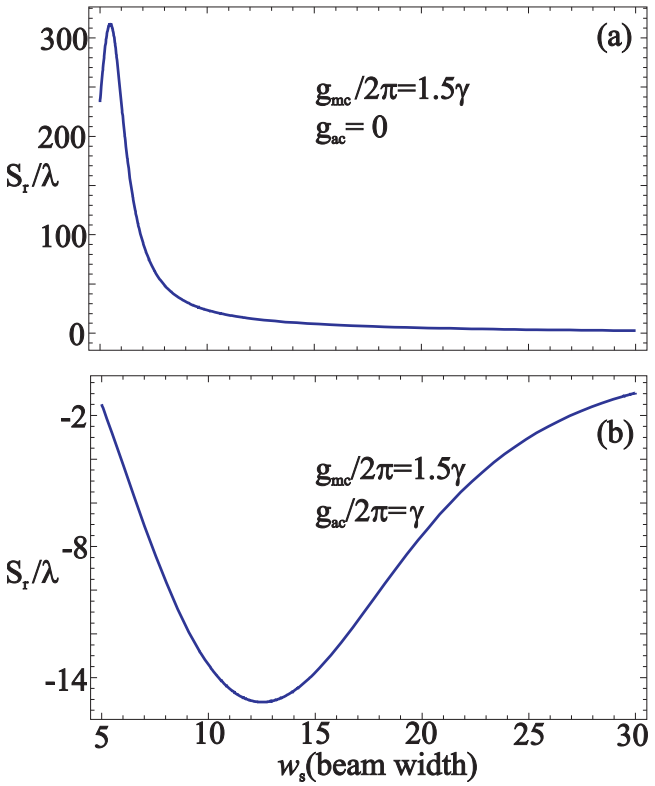

FIG. 7. (a) GH shift vs beam width of Gaussian beam by considering $\theta = 0.46$ rad, $g_{ac} = 0$, and $g_{mc}/2\pi = 1.5\gamma$. (b) The GH shift vs beam width for $\theta = 0.46$ rad, $g_{ac}/2\pi = 1$, and $g_{mc}/2\pi = 1.5\gamma$; the other parameters are $\epsilon_0 = 1$, $\epsilon_1 = 2.22$, $d_1 = 0.2$ μm, $d_2 = 5$ μm, $\gamma = 1$ MHz, $\mathcal{E}_l/2\pi = 0.5\gamma$, $P_l = 4.9$ μW, $\omega_m/2\pi = 10\gamma$, $\Delta_a/2\pi = 10\gamma$, $\gamma_a/2\pi = 0.002\gamma$, $\Gamma_m/2\pi = 0.000\,141\gamma$, and $\kappa = \omega_m/10$.

section, we are going to proceed with the study related to the GH shift by considering that a partially coherent light beam is incident on an OMC. It is established that the quantum parameters such as g_{mc} and g_{ac} affect the behavior of OMIT in a cavity optomechanical system. In the following, we expect the manipulation of the GH shift in the reflected beam via g_{ac}, g_{mc}, beam width w_s, and a measure of global coherence q. Under the influence of g_{ac} and g_{mc}, we plot the GH shift versus incident angle θ for a partially coherent beam using Eq. (21) as shown in Fig. 8. At different incident angles, we get negative and positive GH shifts in the reflected beam. At incident angle $\theta = 0.56$ radian, an enhanced negative GH shift is achieved. The enhanced negative GH shift is achieved which is based on the quantum parameters g_{ac} and g_{mc} as well as a measure of global coherence q and beam width w_s. To study more about the manipulation of the GH shift under the influence of the quantum parameters g_{mc} and g_{ac}, next we consider the fixed incident angle θ and plot the GH shift versus g_{mc} and g_{ac}, separately. First, we consider the incident angle $\theta = 0.56$ radian while ignoring the atom-cavity coupling strength, i.e., $g_{ac} = 0$, and plot the GH shift versus g_{mc} for partial coherent beam as depicted in Fig. 9(a). Interestingly, enhanced negative GH shift ($S_n^r \approx -800$) in the reflected beam is achieved at coupling strength $2\pi g_{mc} = 3.75\gamma$ or $g_{mc} = 0.59\gamma$. Further, to study the influence of g_{ac} on the GH shift, we consider the optomechanical strength $g_{mc} = 0$ and plot the GH shift versus

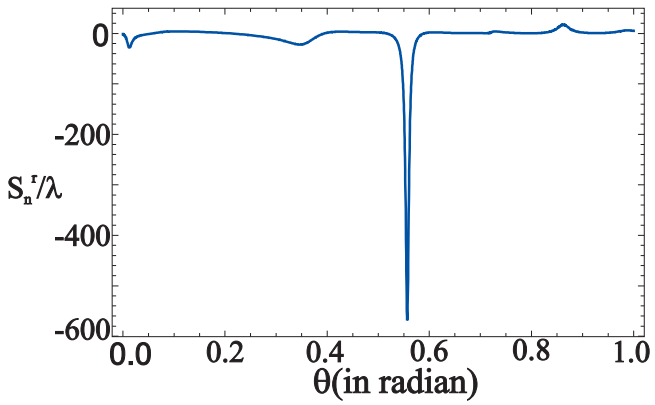

FIG. 8. GH shift vs incident angle θ by considering $g_{ac}/2\pi = g_{mc}/2\pi = \gamma$, nth mode=2, $w_s = 30\lambda$, and $q = 0.013$; the other parameters are $\epsilon_0 = 1$, $\epsilon_1 = 2.22$, $d_1 = 0.2$ μm, $d_2 = 5$ μm, $\gamma = 1$ MHz, $\mathcal{E}_l/2\pi = 0.5\gamma$, $P_l = 4.9$ μW, $\omega_m/2\pi = 10\gamma$, $\Delta_a/2\pi = 10\gamma$, $\gamma_a/2\pi = 0.002\gamma$, $\Gamma_m/2\pi = 0.000\,141\gamma$, $\kappa = \omega_m/10$, and $\delta = 62.82\gamma$.

g_{ac} for a partially coherent beam as shown in Fig. 9(b). It is investigated that the magnitude of the GH shift is approximately zero for small values of g_{ac} and increases gradually with increasing the strength of g_{ac}. We get the increase of

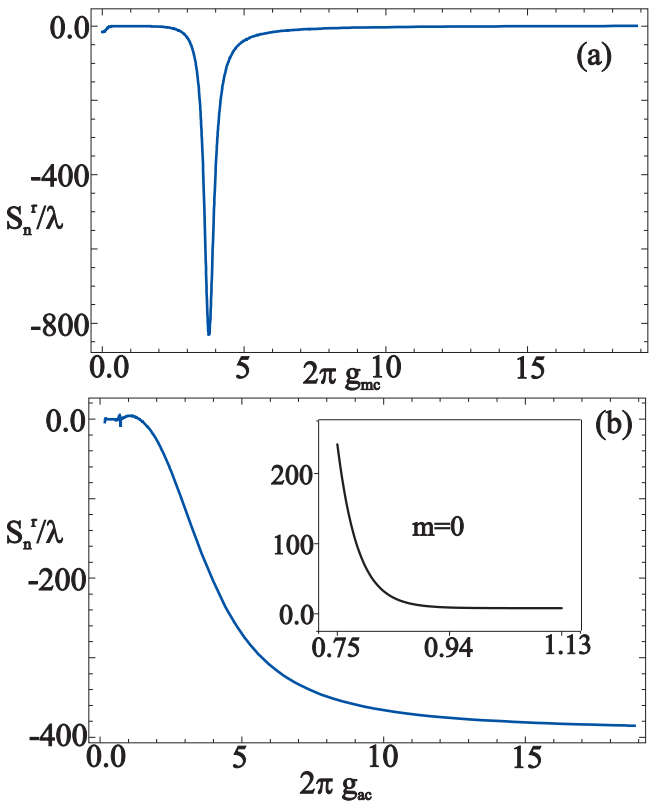

FIG. 9. (a) GH shift vs g_{mc}, where $g_{ac} = 0$, $\theta = 0.56$ rad, $n = 2$, $q = 0.013$, and $w_s = 30\lambda$. (b) The GH shift vs g_{ac}, where $g_{mc} = 0$, $\theta = 0.56$ rad, $n = 2$, $q = 0.013$, and $w_s = 30\lambda$; the other parameters are $\epsilon_0 = 1$, $\epsilon_1 = 2.22$, $d_1 = 0.2$ μm, $d_2 = 5$ μm, $\gamma = 1$ MHz, $\mathcal{E}_l/2\pi = 0.5\gamma$, $P_l = 4.9$ μW, $\omega_m/2\pi = 10\gamma$, $\Delta_a/2\pi = 10\gamma$, $\gamma_a/2\pi = 0.002\gamma$, $\Gamma_m/2\pi = 0.000\,141\gamma$, $\kappa = \omega_m/10$, and $\delta = 62.82\gamma$.

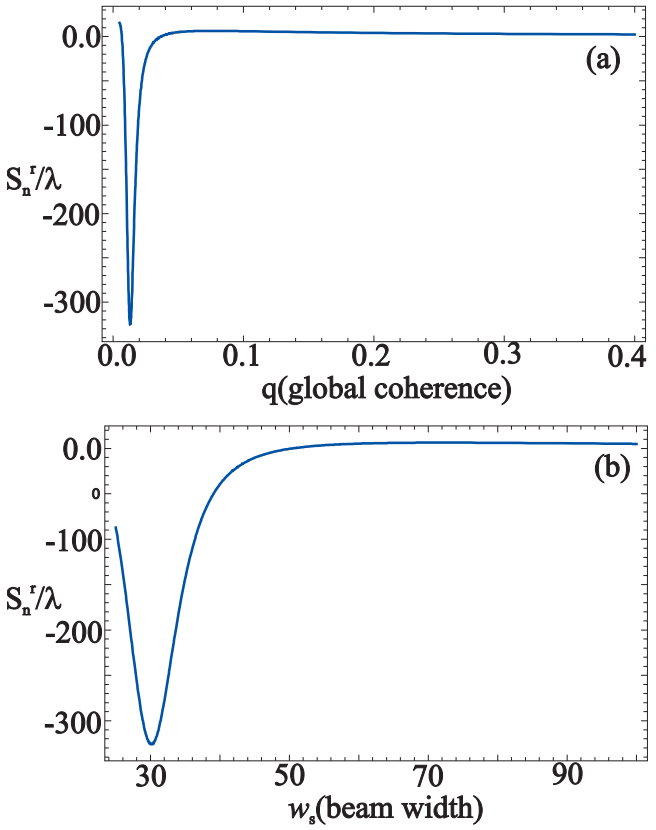

FIG. 10. (a) GH shift vs q, where $g_{ac}/2\pi = g_{mc}/2\pi = \gamma$, $\theta = 0.56$ rad, $n = 2$, and $w_s = 30\lambda$. (b) The GH shift vs w_s, where $g_{ac}/2\pi = g_{mc}/2\pi = \gamma$, $\theta = 0.56$ rad, $n = 2$, and $q = 0.013$; the other parameters are $\epsilon_0 = 1$, $\epsilon_1 = 2.22$, $d_1 = 0.2$ μm, $d_2 = 5$ μm, $\gamma = 1$ MHz, $\mathcal{E}_l/2\pi = 0.5\gamma$, $P_l = 4.9$ μW, $\omega_m/2\pi = 10\gamma$, $\Delta_a/2\pi = 10\gamma$, $\gamma_a/2\pi = 0.002\gamma$, $\Gamma_m/2\pi = 0.000\,141\gamma$, $\kappa = \omega_m/10$, and $\delta = 62.82\gamma$.

the negative GH shift by increasing the value of g_{ac}. This is due to the fact that negative group index (with small values) of the total cavity can be achieved for small values of g_{ac} when a partially coherent beam is propagating through the optomechanical cavity and vice versa.

The negative GH shift becomes maximum around $2\pi g_{ac} = 12\gamma$ or $g_{ac} = 1.9\gamma$. For further increase in the strength of g_{ac}, the magnitude of the negative GH shift remains constant. It has been reported earlier that the mode index n affects the magnitude of the GH shift [21,22]. In Fig. 9(b), we consider the mode index $n = 2$ for partially coherent light and we achieved small GH shift for small values of g_{ac} and vice versa. The behavior of the GH shift changes when the mode index $n = 0$ is considered; see the inset in Fig. 9(b). The result [inset in Fig. 9(b)] reflects the same behavior of the GH shift as we reported for the Gaussian beam where the magnitude of the GH shift is large for small values of g_{ac} and vice versa.

Previously, it has been reported that the spatial coherence of the partially coherent beam influence the magnitude of the GH shift in the reflected beam [21,22]. From these studies, it is revealed that the magnitude of the positive and negative GH shift in the reflected beam is large for small values of q and decreases when the value of q decreases. It is important to emphasize that, for higher values of q, the incident

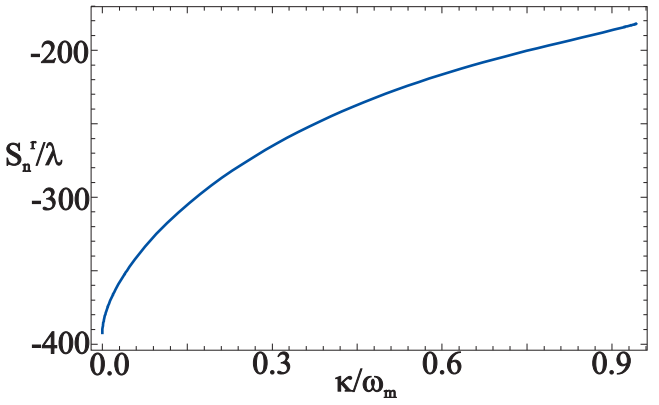

FIG. 11. GH shift vs κ/ω_m, where $g_{ac}/2\pi = g_{mc}/2\pi = \gamma$, $\theta = 0.56$ rad, $n = 2$, and $w_s = 30\lambda$. (b) The GH shift vs w_s, where $g_{ac}/2\pi = g_{mc}/2\pi = \gamma$, $\theta = 0.56$ rad, $n = 2$, and $q = 0.013$; the other parameters are $\epsilon_0 = 1$, $\epsilon_1 = 2.22$, $d_1 = 0.2$ μm, $d_2 = 5$ μm, $\gamma = 1$ MHz, $\mathcal{E}_l/2\pi = 0.5\gamma$, $P_l = 4.9$ μW, $\omega_m/2\pi = 10\gamma$, $\Delta_a/2\pi = 10\gamma$, $\gamma_a/2\pi = 0.002\gamma$, $\Gamma_m/2\pi = 0.000\,141\gamma$, and $\delta = 62.82\gamma$.

beam is more coherent, while for small values it becomes incoherent or partially coherent. To analyze the influence of a measure of global coherence on the magnitude of the GH shift, we consider the incident angle $\theta = 0.56$ radian, the beam width $w_s = 30\lambda$, and plot the GH shift versus q as shown in Fig. 10(a). The spectrum of the GH shift clearly shows that the magnitude becomes maximum at around $q = 0.013$ and decreases with increasing the value of q. It is also reported that the beam width of the Gaussian and partially coherent light plays an important role in the investigation of the GH shift [10,21,22]. It is developed that when the beam width increases, the influence of the partially coherent beam on the GH shift decreases, and vice versa. To study this behavior in OMC, we consider $q = 0.013$ and plot the GH shift versus the beam width of the partially coherent beam; see Fig. 10(b). It is investigated that the magnitude of the GH shift becomes maximum at around $w_s = 30\lambda$ and decreases for further increase in the beam width of the partially coherent beam.

Besides, the cavity decay is very important and it is necessary to study its effect on the GH shift. The cavity decay is different for different cavities and depends upon the Q factor. The cavity decay can influence the OMIT and the reflection coefficient. The expression of the GH shift is directly dependent on the reflection coefficient. Therefore, the GH shift in the reflected beam must be affected. To study the effect, we consider the measure of global coherence $q = 0.013$ and the beam width $w_s = 30\lambda$ of the partially coherent beam and plot the GH shift versus decay rate κ as depicted in Fig. 11. The plot shows that when the cavity decays, i.e., $\kappa/\omega_m = 0$, we get maximum negative GH shift. The magnitude of the GH shift decreases with increasing the value of κ. This means that, for a very lossy medium, the magnitude of the GH shift will remain small and vice versa. Throughout our analysis, we consider the decay rate, i.e., $\kappa/\omega_m = 0.1$.

IV. SUMMARY

In summary, we propose a scheme to greatly enhance the GH shift by using the OMC system. In the first part of this

work, we studied the GH shift in the reflected beam when the input probe beam is Gaussian shape. The GH shift can be enhanced by the proper control of the two quantum parameters g_{mc} and g_{ac}. Besides, the influence of the input beam width is also discussed. In the second part, we study the GH shift with the partially coherent beam in the OMC system. Both the two quantum parameters can affect the GH shift in the mode of $n = 2$, and the magnitude of the GH shift is also affected by the beam width and the measure of global coherence. The scheme is a good system to study the behavior of GH shift on one hand, and also provide an alternative way to estimate the quantum coupling strength by measuring the tiny GH shift.

[1] J. Picht, Ann. Phys. (Paris) **395**, 433 (1929).
[2] F. Goos and H. Hanchen, Ann. Phys. (NY) **436**, 333 (1947).
[3] C.-W. Chen, W.-C. Lin, L.-S. Liao, Z.-H. Lin, H.-P. Chiang, P.-T. Leung, E. Sijercic, and W.-S. Tse, Appl. Opt. **46**, 5347 (2007).
[4] X. Yin and L. Hesselink, Appl. Phys. Lett. **89**, 261108 (2006).
[5] R. H. Renard, J. Opt. Soc. Am. **54**, 1190 (1964).
[6] D. K. Qing and G. Chen, Opt. Lett. **29**, 872 (2004).
[7] T. Tamir and H. L. Bertoni, J. Opt. Soc. Am. **61**, 1397 (1971).
[8] S. Chu and S. Wong, Phys. Rev. Lett. **48**, 738 (1982); J. L. Birman, D. N. Pattanayak, and A. Puri, *ibid.* **50**, 1664 (1983).
[9] P. R. Berman, Phys. Rev. E **66**, 067603 (2002); A. Lakhtakia, Electromagnetics **23**, 71 (2003).
[10] Ziauddin and S. Qamar, Phys. Rev. A **85**, 055804 (2012).
[11] L. G. Wang, M. Ikram, and M. S. Zubairy, Phys. Rev. A **77**, 023811 (2008).
[12] Ziauddin, S. Qamar, and M. S. Zubairy, Phys. Rev. A **81**, 023821 (2010).
[13] Ziauddin and Qamar, Phys. Rev. A **84**, 053844 (2011).
[14] Ziauddin, S. Qamar, and M. Abbas, Laser Phys. Lett. **11**, 015201 (2014).
[15] Ziauddin and S. Qamar, Opt. Commun. **319**, 1 (2014).
[16] A. Aiello and J. P. Woerdman, Opt. Lett. **36**, 3151 (2011).
[17] W. Löffler, A. Aiello, and J. P. Woerdman, Phys. Rev. Lett. **109**, 213901 (2012).
[18] M. Merano, G. Umbriaco, and G. Mistura, Phys. Rev. A **86**, 033842 (2012).
[19] L.-Q. Wang, L.-G. Wang, S.-Y. Zhu, and M. S. Zubairy, J. Phys. B **41**, 055401 (2008).
[20] L.-G. Wang, S. Y. Zhu and M. S. Zubairy, arXiv:1304.5585.
[21] L.-G. Wang, S. Y. Zhu, and M. S. Zubairy, Phys. Rev. Lett. **111**, 223901 (2013).
[22] Ziauddin, Y.-L. Chuang, and R.-K. Lee, Phys. Rev. A **91**, 013803 (2015).
[23] E. Pfleghaar, A. Marseille, and A. Weis, Phys. Rev. Lett. **70**, 2281 (1993).
[24] R. Yang, W. Zhu, and J. Li, Opt. Express **22**, 2043 (2014).
[25] Y. Wan, Z. Zheng, W. Kong, X. Zhao, Y. Liu, Y. Bian, and J. Liu, Opt. Express **20**, 8998 (2012).
[26] I. V. Soboleva, V. V. Moskalenko, and A. A. Fedyanin, Phys. Rev. Lett. **108**, 123901 (2012).
[27] C.-W. Chen, T. Bian, H.-P. Chiang, and P. T. Leung, J. Opt. **18**, 025104 (2016).
[28] Y. Xu, C. T. Chan, and H. Chen, Sci. Rep. **5**, 8681 (2015).
[29] C. Bonnet, D. Chauvat, O. Emile, F. Bretenaker, and A. Le Floch, Opt. Lett. **26**, 666 (2001).
[30] X. Yin, L. Hesselink, Z. Liu, N. Fang, and X. Zhang, Appl. Phys. Lett. **85**, 372 (2004).
[31] Ziauddin, J. Mod. Opt. **62**, 16602015.
[32] Ziauddin, Y.-L. Chuang, and R.-K. Lee, Phys. Rev. A **92**, 013815 (2015).
[33] T. J. Kippenber and J. K. Vahala, Opt. Express **15**, 17172 (2007).
[34] M. Aspelmeyer, T. J. Kippenberg, and F. Marquardt, Rev. Mod. Phys. **86**, 1391 (2014).
[35] G. S. Agarwal and S. Huang, Phys. Rev. A **81**, 041803(R) (2010).
[36] S. Weis *et al.*, Science **330**, 1520 (2010).
[37] J. B. Khurgin, M. W. Pruessner, T. H. Stievater, and W. S. Rabinovich, Phys. Rev. Lett. **108**, 223904 (2012).
[38] E. Verhagen, S. Deléglise, S. Weis, A. Schliesser, and T. J. Kippenberg, Nature (London) **482**, 63 (2012).
[39] H. Xiong, L. G. Si, A. S. Zheng, X. Yang, and Y. Wu, Phys. Rev. A **86**, 013815 (2012).
[40] M. Karuza, C. Biancofiore, M. Bawaj, C. Molinelli, M. Galassi, R. Natali, P. Tombesi, G. DiGiuseppe, and D. Vitali, Phys. Rev. A **88**, 013804 (2013).
[41] D. E. Chang, A. H. Safavi-Naeini, M. Hafezi, and O. Painter, New J. Phys. **13**, 023003 (2011).
[42] J. Q. Zhang, Y. Li, M. Feng, and Y. Xu, Phys. Rev. A **86**, 053806 (2012).
[43] Q. Wang, J. Q. Zhang, P. C. Ma, C. M. Yao, and M. Feng, Phys. Rev. A **91**, 063827 (2015).
[44] K. Stannigel, P. Komar, S. J. M. Habraken, S. D. Bennett, M. D. Lukin, P. Zoller, and P. Rabl, Phys. Rev. Lett. **109**, 013603 (2012).
[45] P. Komar, S. D. Bennett, K. Stannigel, S. J. M. Habraken, P. Rabl, P. Zoller, and M. D. Lukin, Phys. Rev. A **87**, 013839 (2013).
[46] H. Xiong, L. G. Si, and Y. Wu, Appl. Phys. Lett. **107**, 091116 (2015).
[47] H. Xiong, C. Kong, X. Yang, and Y. Wu, Opt. Lett. **41**, 4316 (2016).
[48] T. P. Purdy, P.-L. Yu, R. W. Peterson, N. S. Kampel, and C. A. Regal, Phys. Rev. X **3**, 031012 (2013).
[49] S. Groblacher, K. Hammerer, M. R. Vanner *et al.*, Nature (London) **460**, 724 (2009).
[50] S. E. Harris, J. E. Field, and A. Imamoglu, Phys. Rev. Lett. **64**, 1107 (1990).
[51] G. S. Agarwal and S. Huang, New J. Phys. **16**, 033023 (2014).
[52] U. Fano, Phys. Rev. **124**, 1866 (1961); C. Ott, A. Kaldun, P. Raith, K. Meyer, M. Laux, J. Evers, C. H. Keitel, C. H. Greene, and T. Pfeifer, Science **340**, 716 (2013).
[53] L. Zhang and J. Evers, Phys. Rev. A **90**, 023826 (2014).
[54] K. Yinga, Y. Niub, D. Chena, H. Caia, R. Qua, and S. Gongb, J. Mod. Opt. **61**, 631 (2014).
[55] L. Safari, D. Iablonskyi, and F. Fratini, Eur. Phys. J. D **68**, 1 (2014).

[56] Y. Chen, X. G. Wei, and B. S. Ham, J. Phys. B: At., Mol., Opt. Phys. **42**, 065506 (2009).
[57] B. P. Hou, S. J. Wang, W. L. Yu, and W. L. Sun, Phys. Lett. A **352**, 462 (2006).
[58] P. C. Ma, J. Q. Zhang, and Y. Xiao, M. Feng and Z. M. Zhang, Phys. Rev. A **90**, 043825 (2014).
[59] S. Jing, Chin. Phys. Lett. **28**, 104203 (2011).
[60] W. J. Gu and Z. Yi, Opt. Commun. **333**, 261 (2014).
[61] S. Shahidani, M. H. Naderi, and M. Soltanolkotabi, Phys. Rev. A **88**, 053813 (2013).
[62] Ziauddin, Mujeeb-ur-Rahman, I. Ahmad, and S. Qamar, Europhys. Lett. **120**, 24001 (2017).
[63] A. Schliesser and T. J. Kippenberg, Physics **4**, 97 (2011).
[64] J. Restrepo, C. Ciuti, and I. Favero, Phys. Rev. Lett. **112**, 013601 (2014).
[65] S. Haroche and D. Kleppner, Phys. Today **42**(1), 24 (1989).
[66] T. J. Kippenberg and K. J. Vahala, Science **321**, 1172 (2008).
[67] K. Hammerer, M. Wallquist, C. Genes, M. Ludwig, F. Marquardt, P. Treutlein, P. Zoller, J. Ye, and H. J. Kimble, Phys. Rev. Lett. **103**, 063005 (2009).
[68] M. J. Akram, M. M. Khan, and F. Saif, Phys. Rev. A **92**, 023846 (2015).
[69] R. A. Norte, J. P. Moura, and S. Gröblacher, Phsy. Rev. Lett. **116**, 147202 (2016).
[70] G. De Chiara, M. Paternostro, and G. M. Palma, Phys. Rev. A **83**, 052324 (2011).
[71] M. Ullah, A. Abbas, J. Jing, and L.-G. Wang, Phys. Rev. A **100**, 063833 (2019).
[72] S. Haroche and J. M. Raimond, *Exploring the Quantum: Atoms, Cavities, and Photons* (Oxford University, Oxford, 2006).
[73] M. J. Akram, F. Ghafoor, and F. Saif, J. Phys. B **48**, 065502 (2015).
[74] D. F. Walls and G. J. Milburn, *Quantum Optics* (Springer, New York, 2008).
[75] L.-G. Wang and S.-Y. Zhu, Opt. Lett. **31**, 101 (2006).
[76] L. Mandel, and E. Wolf, *Optical Coherence and Quantum Optics* (Cambridge University Press, Cambridge, England, 1995).
[77] H. Ian, Z. R. Gong, Y. X. Liu, C. P. Sun, and F. Nori, Phys. Rev. A **78**, 013824 (2008).